

Analysis of Failure Waves with an Elasto-statistical-brittle Model

Zhijie Jiang¹, Mengfen Xia¹, Haiying Wang^{1,*}

¹ Institute of Mechanics, Chinese Academy of Sciences, 100190, China

* Corresponding author: why@lm.imech.ac.cn

Abstract The origin and propagation mechanism of failure waves poses a challenge to our conventional understanding of dynamic failure. In this paper, the failure wave is attributed to the catastrophic rupture in brittle materials and an elasto-statistical-brittle (ESB) model is developed to describe the catastrophic behavior. In the ESB model, the disordered heterogeneity of brittle solids at mesoscopic scale is characterized with statistical description of the shear strength of mesoscopic units. The evolution of microdamage is controlled by the shear strength and the shear stress applied, and eventually induces catastrophic rupture in brittle materials. Considering the failure wave as a propagating boundary of catastrophic failure, the propagation of the failure wave is predicated with wave theory. Several predicted speeds of failure waves are in good agreement with experimental observations.

Keywords failure wave, wave speed, elasto-statistical-brittle model, catastrophic rupture, heterogeneity

1. Introduction

Shock induced delayed failure (the so called failure wave) in brittle materials has attracted extensive research in recent years [1-11]. This feature was first noted by Razorenov et al [2] as a small reload signal superimposed on rear surface velocity trace, suggesting the interaction of the release from the rear surface of the target with a moving front behind which the material undergoes a reduction of shock impedance. Further experiments [3] prove that the failure wave can be generated in glasses or ceramics at a stress near or below the HEL and the speed of failure wave does not correspond to any elastic wave. In addition, behind this wave, the longitudinal stress changes little but the transverse stress increases, indicating a decrease in shear strength, and spall tensile strength falls to essentially zero [4-6].

Several models have been proposed to address the origin of failure waves. However, a satisfactory explanation and description for the failure wave is still lacking. Clifton [7] assumes the failure wave as a propagating phase boundary. In his model, the square of the failure wave speed is proportional to the ratio of the jump in stress over the jump in strain. However, the available stress measurements clearly show that the failure wave causes either no change or small deduction in the longitudinal stress, but a large jump in the longitudinal strain. Feng [8] suggests that the propagation mechanism of failure front is a diffusive process. In his model, the failure front is not a mechanical wave, and the failure front speed is controlled by the stress deviator and dilated volume. To some extent, his simulation agrees with experiments, but the failure wave speed is disordered during the failure wave propagating. Moreover, his model assumes no changes in the longitudinal strain, which conflicts with experimental observations [9]. Kanel [2], Partom [10] and Espinosa [11] suppose the failure wave as a damage evolution process originating from the shocked surface. Hence, the predicted failure evolution behind the initial shock wave is independent of location instead of having an increasing time delay with propagation distance as observed experimentally. As a result, the simulations of the failure wave phenomenon based on this type of material model require the use of a nonphysical “failure wave”, e.g. switching on a failure process cell by cell at an assumed successive sequence.

In this paper, we attribute the failure wave to a propagating catastrophe process in brittle materials. To describe catastrophic rupture in heterogeneous brittle materials, an elasto-statistical-brittle (ESB)

model is developed. Considering the failure wave as a propagating boundary of catastrophic failure, the critical condition to generate failure wave and the failure wave speed could be obtained from the law of conservation.

The paper is organized as follows: Section 2 describes the details of ESB model and Section 3 is the modelling of failure wave phenomenon. Numerical simulation and comparison with the experimental data are presented in Section 4. A summary is given in Section 5.

2. Elasto-statistical-brittle (ESB) MODEL

Generally speaking, the catastrophic failure of heterogeneous brittle materials under impact loading is resulted from the initiation, growth, and coalescence of microdamage, which is obviously controlled by the interactions of stress pulse with local material properties and microstructure. Hence, in the ESB model, we consider a macroscopic representative volume element (RVE) comprised of a great number of heterogeneous mesoscopic units. The heterogeneity of the mesoscopic units can be characterized by their shear strength. For instance, we assume their shear strength τ_c follows a statistical distribution $h(\tau_c)$. The Weibull distribution is often used in the field of failure analysis due to its flexibility. That is,

$$h(\tau_c) = \frac{m}{\eta} \left(\frac{\tau_c}{\eta}\right)^{m-1} \exp\left(-\left(\frac{\tau_c}{\eta}\right)^m\right) \quad (1)$$

where η and m are the scale parameter and shape parameter of Weibull distribution, respectively. The scale parameter η is proportional to the mean strength of mesoscopic units and the shape parameter m reflects the degree of material heterogeneity. Physically, a larger m implies a more homogeneous material. Fig. 1 shows the distribution of material shear strength with different heterogeneity index m .

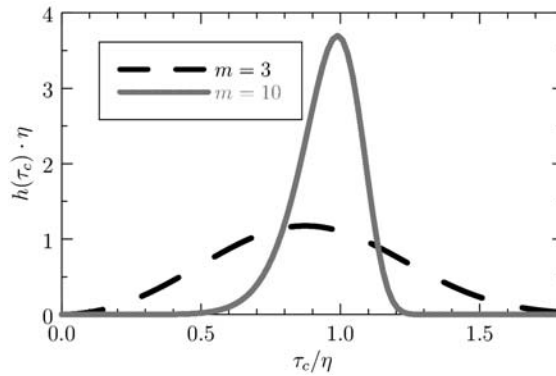


Figure 1. The distribution of material shear strength with different shape parameter m

If the applied shear stress on the mesoscopic unit τ_{meso} reaches its shear strength τ_c , the unit fails. Denote macroscopic damage of the RVE as D , which can be expressed as:

$$D = \int_0^{\tau_{meso}} h(\tau_c) d\tau_c = 1 - \exp\left(-\left(\tau_{meso}/\eta\right)^m\right) \quad (2)$$

We further assume that compared with intact unit, the breaking mesoscopic units can sustain less hydrostatic stress but no shear stress. This assumption physically means that the macroscopic damage causes reductions in both shear modulus and volumetric modulus of the material, and the latter degrades less than the former. That is,

$$\begin{aligned} G &= G_0(1-D) \\ K &= (1-\zeta D)K_0 \end{aligned} \quad (3)$$

where $\zeta < 1$, K_0 and G_0 are the volumetric modulus and shear modulus of intact material, respectively.

The material behavior at the macroscopic level can be written as

$$\sigma_{ij} = [1 - \zeta + \zeta \exp(-(\tau_{meso}/\eta)^m)] K_0 \theta \delta_{ij} + 2G_0 \exp(-(\tau_{meso}/\eta)^m) (\varepsilon_{ij} - \frac{1}{3} \theta \delta_{ij}) \quad (4)$$

where ε_{ij} is the strain tensor, σ_{ij} the stress tensor, θ the volumetric strain. Provided small damage and mean field approximation, γ is the maximum shear strain of the macroscopic element. Hence,

$$\tau_{meso} = G_0 \gamma. \quad (5)$$

Specifically, in uniaxial strain state ($\varepsilon_x = \gamma \neq 0$, $\varepsilon_y = \varepsilon_z = 0$), the constitutive relation can be simplified as

$$\begin{aligned} \sigma_x &= [1 - \zeta + \zeta \exp(-(G_0 \varepsilon_x / \eta)^m)] K_0 \varepsilon_x + \frac{4}{3} G_0 \exp(-(G_0 \varepsilon_x / \eta)^m) \varepsilon_x \\ \sigma_y &= [1 - \zeta + \zeta \exp(-(G_0 \varepsilon_x / \eta)^m)] K_0 \varepsilon_x - \frac{2}{3} G_0 \exp(-(G_0 \varepsilon_x / \eta)^m) \varepsilon_x \\ \tau_{xy} &= G_0 \exp(-(G_0 \varepsilon_x / \eta)^m) \varepsilon_x \end{aligned} \quad (6)$$

In order to show the response of material under impact, we normalize the constitutive relation and get the dimensionless constitutive relation as

$$\begin{aligned} \bar{\sigma}_x &= \frac{2(1+\nu)}{3(1-2\nu)} [1 - \zeta + \zeta \exp(-\bar{\varepsilon}_x^m)] \bar{\varepsilon}_x + \frac{4}{3} \bar{\varepsilon}_x \exp(-\bar{\varepsilon}_x^m) \\ \bar{\sigma}_y &= \frac{2(1+\nu)}{3(1-2\nu)} [1 - \zeta + \zeta \exp(-\bar{\varepsilon}_x^m)] \bar{\varepsilon}_x - \frac{2}{3} \bar{\varepsilon}_x \exp(-\bar{\varepsilon}_x^m) \\ \bar{\tau}_{xy} &= \bar{\varepsilon}_x \exp(-\bar{\varepsilon}_x^m) \end{aligned} \quad (7)$$

where ν is the Poisson's ratio of the intact material, $\bar{\sigma}_{ii} = \sigma_{ii}/\eta$, $\bar{\varepsilon}_{ii} = G_0 \varepsilon_{ii}/\eta$. Fig.2 plots the normalized stress-strain relationship with different parameters.

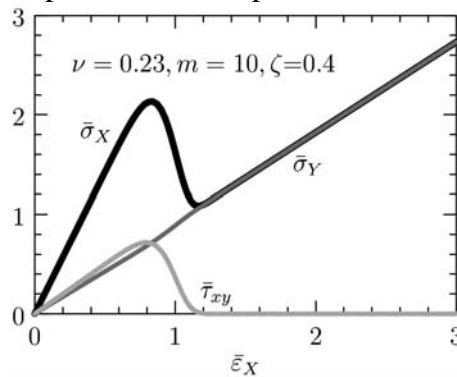


Figure 2. The simplified stress-strain relationship in uniaxial strain state

As Fig.2 shows, there exists a saddle point in the $\varepsilon_x - \sigma_x$ curve. Actually, the saddle point implies a catastrophic transition happening. As illustrated in Fig.3, when the longitudinal stress reaches σ_E , solids can not sustain any further compression, all of the meso-elements fail suddenly and the state directly jump from the unstable state A to the corresponding state B. In this process, the energy provided is used in fragmenting, thus, the longitudinal stress does not change.

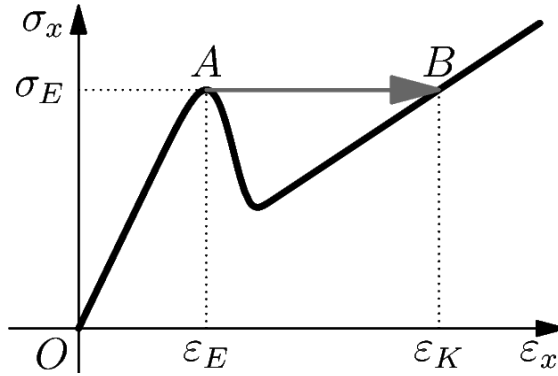


Figure 3. The catastrophic transition in ESB model

3. MODELLING OF THE FAILURE WAVE

In this section, we will analyze the origin of failure waves in a target plate described with a simplified ESB model.

Fig. 4 is the $x-t$ diagram of flyer plate and target plate. In the flyer plate, region 1 is in the initial state and region 4 in the final state. In the target plate, region 2 is the shocked region behind the elastic wave and region 3 is failed zone behind the failure wave. As the flyer plate and target plate do not split up, region 3 and region 4 have the same longitudinal stress and particle velocity.

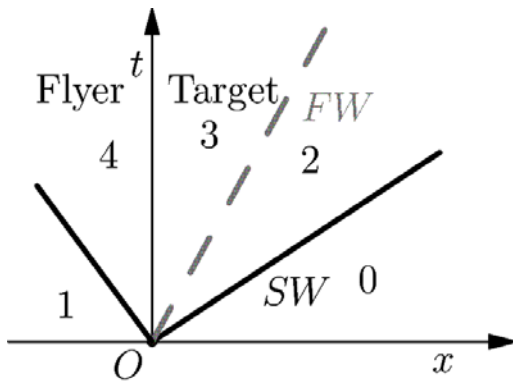


Figure 4. the $x-t$ diagram for waves

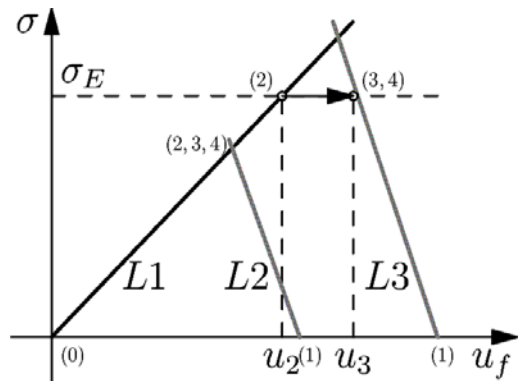


Figure 5. the $u-\sigma$ plane of plates system

Fig. 5 is the $u-\sigma$ plane of plates system. In the $u-\sigma$ plane, (u_2, σ_E) stands for region 2, and (u_3, σ_E) stands for region 3 and 4. L1 is the trajectory of states in flyer plate, and L2 is the trajectory of states of target subjected to low-velocity impact. When the impact loading is lower than the stress threshold σ_E , the catastrophic transition couldn't happen and there is no failure wave. However, if the stress state of target could exceed the stress threshold σ_E , as expressed by

L3 and L1, the catastrophic rupture happens and failure wave comes out.

Considering the law of conservation of mass, the failure wave speed can be obtained as,

$$C_{fw} = \frac{u_3 - u_2}{\varepsilon_3 - \varepsilon_2} = \frac{u_f - \rho_f \varepsilon_{fE} - \rho_t \varepsilon_2}{\varepsilon_3 - \varepsilon_2} \quad (8)$$

4. NUMERICAL SIMULATION

In order to validate our theory, we simulate normal impact experiments on soda-lime glass specimens by copper plates. The properties of copper and soda-lime glass are summarized in Table 1.

Table 1 The properties of flyer plate materials [3]

Material	$C_L / km \cdot s^{-1}$	$\rho / kg \cdot m^{-3}$	ν
copper	4.560	8930	0.33
soda-lime glass	5.840	2490	0.23

Bourne et al. [3, 12] studied failure waves in soda-lime glass impacted with copper flyer. The results prove that the threshold stress to generate failure wave in soda-lime glass is 4.0 GPa. Therefore, in the simulation, we assume the threshold stress σ_E to be 4.0 GPa. In addition, since soda-lime glass is less heterogeneous, the shape parameter m is set as 10 and ζ as 0.4. The stress-strain relationship of soda-lime glass is presented in Fig. 6. As Fig. 6 shows, for soda-lime glass, the strain at the threshold stress is 0.0471 prior to the catastrophic rupture (ε_E) and 0.1330 after the catastrophic rupture (ε_K). With these parameters, we can calculate the speed of failure waves from Eq. (8).

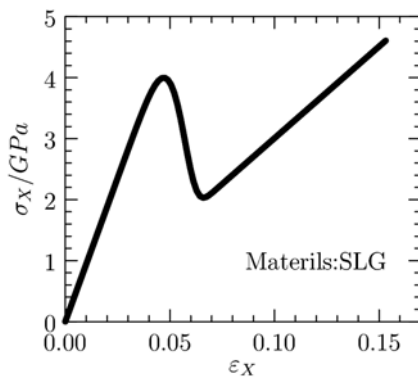


Figure 6. The response of soda-lime glass

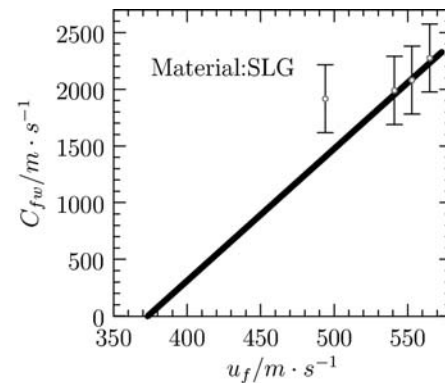


Figure 7. The relationship between u_f and C_{fw}

From Eq. (8), we obtain the relationship of failure wave speed vs. the impact velocity, as shown in Fig.7. It is obvious that, according to the ESB model, the speed of failure wave is linear with the impact velocity. In addition, Fig.7 demonstrates that the lowest impact velocity to generate the failure wave is 373.3 m/s, which approximately coincides with experimental observations [3, 12]. Table 2 quantitatively compares the speed of failure waves calculated with the ESB model with

experimental ones. Apparently, the model can basically replicate the experiments and the error is acceptable.

Table 2. Summary of Experimental data and the simulation results [3, 12]

Shot no.	Impactor	Target	Impact velocity u_f	C_{fw} (experimental)	C_{fw} (simulated)
98-01	copper	soda lime glass	494 m/s	1916 ± 300 m/s	1405 m/s
98-02	copper	soda lime glass	541 m/s	1989 ± 300 m/s	1952 m/s
98-03	copper	soda lime glass	553 m/s	2080 ± 300 m/s	2092 m/s
98-04	copper	soda lime glass	565 m/s	2275 ± 300 m/s	2232 m/s

5. SUMMARY

The origin and propagation of failure waves in brittle materials under impact loading have been investigated for many years. However, till now, failure waves cannot be well illustrated by any constitutive models. In this paper, the failure wave is attributed to the catastrophic rupture in brittle materials under impact loading. To describe the catastrophe behavior, an elasto-statistical-brittle (ESB) model is developed. In the ESB model, the shear strength of mesoscopic units follows a Weibull distribution, which reflects the heterogeneity of brittle solids. The evolution of microdamage is controlled by the shear strength and the shear stress applied, and induces reductions in shear modulus and volumetric modulus. Catastrophic rupture occurs when stress cannot be hold by the damaged material.

With the ESB model and wave theory, we predicted the failure waves in soda-lime glass impacted with copper plates. The critical impact velocity to generate the failure wave approximately coincides with experimental data. In addition, several predicted speeds of failure waves are in good agreement with experimental observations.

Acknowledgements

This work was supported by the National Natural Science Foundation of China (Grant Nos. 11172311, 11021262, 10932011).

References

- [1] S. J. Bless and N. S. Brar, failure wave and their effects on penetration mechanics in glass and ceramics, in: Y. Horie(Eds.), Shock Wave Science and Technology Reference Library, Springer, New York, 2007, pp. 105-141.
- [2] G. I. Kanel, S. V. Rasorenov and V. E. Fortov, The failure waves and spallations in homogeneous brittle materials, in: S. C. Schmidt, R. D. Dick and J. W. Forbes(Eds.), Shock Compression of Condensed Matter, Elsevier, New York, 1991, pp. 451-454.
- [3] N. Bourne, J. Millett, Z. Rosenberg and N. Murray, On the shock induced failure of brittle solids, Journal of the Mechanics and Physics of Solids, 46(1998) 1887-1908.
- [4] N. S. Brar, S. J. Bless and Z. Rosenberg, Impact-induced failure waves in glass bars and plates, Applied Physics Letters, 56(1991) 3396-3398.
- [5] N. S. Brar, Z. Rosenberg and S. J. Bless, Spall strength and failure waves in glass, Journal De Physique IV, 1(1991) 639-644.
- [6] H. D. Espinosa and Y. P. Xu, Micromechanics of Failure Waves in Glass: I, Experiments,

- Journal of the American Ceramic Society, 80(1997) 2061-2073.
- [7] R. J. Clifton, Analysis of Failure Waves in Glasses, *Applied Mechanics Reviews*, 46(1993) 540-546.
 - [8] R. Feng, Formation and propagation of failure in shocked glasses, *Journal of Applied Physics*, 87(2000) 1693-1700.
 - [9] Z. Rosenberg, N. K. Bourne and J. C. F. Millett, Direct measurements of strain in shock-loaded glass specimens, *Journal of Applied Physics*, 79(1996) 3971-3974.
 - [10] Y. Partom, Modeling failure waves in glass, *International Journal of Impact Engineering*, 21(1998) 791-799.
 - [11] H. D. Espinosa, Y. P. Xu and N. S. Brar, Micromechanics of Failure Waves in Glass: II, Modeling, *Journal of the American Ceramic Society*, 80(1997) 2074-2085.
 - [12] J. C. F. Millett and N. K. Bourne, Effect of internal strain on the propagation of failure in shock loaded soda-lime glass, *Journal of Applied Physics*, 95(2004) 4681-4685.